Heliyon 10 (2024) e25015

Contents lists available at ScienceDirect

Heliyon

journal homepage: www.cell.com/heliyon

Research article

Thermal, thermomechanical and structural properties of recycled polyethylene terephthalate (rPET)/waste marble dust composites

László Lendvai [a], Tej Singh [b,*], Ferenc Ronkay [c]

[a] Department of Materials Science and Engineering, Széchenyi István University, H-9026, Győr, Hungary
[b] Savaria Institute of Technology, Faculty of Informatics, ELTE Eötvös Loránd University, Budapest, 1117, Hungary
[c] Department of Innovative Vehicles and Materials, GAMF Faculty of Engineering and Computer Science, John von Neumann University, H-6000, Kecskemét, Hungary

ARTICLE INFO

Keywords:
Recycled polyethylene terephthalate
rPET
Marble dust
Thermal properties
Composites

ABSTRACT

The main objective of this work is to review the capability of using waste marble dust (MD) particles as reinforcing materials in recycled polymeric composites to achieve environmentally friendly materials. In the present study, polymer composites were fabricated from recycled polyethylene terephthalate (rPET) and MD and then analyzed for their structural and thermal properties. Preparation of rPET-based composites containing 0–20 wt% MD was carried out through extrusion and injection molding. For their characterization Fourier transform infrared spectroscopy (FTIR), differential scanning calorimetry (DSC), thermogravimetric analysis (TGA), and dynamic mechanical analysis (DMA) were applied. The DSC analysis revealed a nucleating effect of MD on rPET, which was manifested in a higher crystallization temperature (196.7 °C ⇒ 204.4 °C); however, the marble particles were also found to hamper chain mobility, thereby decreasing the crystallinity ratio (23.7 % ⇒ 19.2 %) of rPET and altering its crystalline structure. According to the TGA measurements, a slight increase occurred in the thermal stability of rPET, its major decomposition temperature increased from 446 °C to 451 °C when 20 wt% MD was incorporated into it. DMA showed an improved stiffness in the entire investigated temperature range for MD-filled composites versus neat rPET. Additionally, several factors were derived from the DMA data, including the effectiveness factor, degree of entanglement, and reinforcing efficiency factor which all suggested a decent interaction between the components indicating a proper reinforcing ability of marble powder. However, above 5 wt% MD content the reinforcing efficiency deteriorated due to the agglomeration of filler particles, which was also supported by scanning electron microscopic images.

1. Introduction

The utilization of waste resources in the manufacturing industry is becoming increasingly common [1]. Utilizing waste resources does not only help to reduce the environmental burden associated with their disposal but also proves helpful in developing low-cost products and encourages sustainability [2]. Furthermore, the use of waste materials follows the concept of circular economy, which seeks to finish the loop by reusing discarded materials rather than adhering to a linear model where resources are harvested, utilized, and then discarded [3]. A circular economy promotes system enhancements to eliminate waste, better use of resources, and to establish

* Corresponding author.
E-mail address: sht@inf.elte.hu (T. Singh).

https://doi.org/10.1016/j.heliyon.2024.e25015
Received 10 September 2023; Received in revised form 27 December 2023; Accepted 18 January 2024
Available online 19 January 2024

a more sustainable equilibrium between the environment, the economy, and society [4,5]. Marble, a metamorphic rock composed of recrystallized dolomite ($CaMg(CO_3)_2$) or calcite ($CaCO_3$), has long been prized for its numerous applications, including in sculpting, architecture, and decorative arts [6–8]. Nevertheless, excavating useable marble from the quarry and its subsequent factory processing generates enormous waste, almost 75 % of the overall output according to some estimations [8]. Approximately 200 million tons of marble processing residues are estimated to be discarded as waste annually, causing social, environmental, and economic problems [9]. Because of the growing environmental concerns caused by waste materials and the rigorous restrictions governing their disposal, researchers are increasingly incentivized to employ marble waste in developing new innovative products. According to studies, marble waste may be applied to various industries, including glass, agriculture, paper, and construction [6–10]. Using waste properly may decrease pollution, and the planet can become cleaner and "greener". Using marble waste to replace conventional fillers in developing polymer composites can be alluring. The chemical composition of waste marble, which includes conventional additives such as silicon dioxide, aluminum oxide, and calcium oxide, bolsters its utility in developing sustainable composites [6,7].

The utilization of marble dust (MD) and polyethylene terephthalate (PET) was investigated by Çınar and Kar [11] in their study on producing eco-friendly polymer composites. According to their findings, higher amounts of MD resulted in enhanced stiffness, hardness, thermal conductivity, and bending strength of the developed composites. In their research, Bakshi et al. [12] investigated the viability of integrating marble waste in different amounts to produce polypropylene-based composites. The researchers emphasize that the desired density and mechanical properties can be attained by carefully selecting the appropriate marble waste loading and molding temperature parameters. The influence of incorporating MD at different weight percentages (0 %, 10 %, 20 %, and 30 %) on the mechanical and thermal characteristics of glass fiber-reinforced epoxy composites was examined by Choudhary et al. [13]. Their findings suggest that including MD increased the fabricated composites' hardness, crystallinity, thermal conductivity, and dynamic mechanical properties. Among mechanical properties, tensile strength decreased, while fracture toughness and inter-laminar shear strength increased with an increased MD loading. In contrast, the composites' flexural modulus, tensile modulus, and flexural strength exhibited an upward trend up to an MD content of 20 %. On the other hand, it decreased when higher amounts of MD were added. By employing a decision-making technique, the authors determined that 20 % MD dosage is adequate for achieving the optimal combination of the evaluated properties. Nayak and Satapathy [14] conducted a study in which they developed polyester-based composites utilizing waste MD for engineering applications related to wear. The research examined the influence of marble particle size (ranging from 58 to 155 μm) and loading level (0–40 % by weight). The findings revealed that when the particle size or weight percentage of MD increased, the properties of the produced composites, including compressive strength, impact energy, and hardness, also increased. The research by Sharma et al. [15] focused on the impact of incorporating MD at varying weight percentages (ranging from 0 % to 24 %) on jute fiber-reinforced epoxy composites' mechanical and thermal properties. The findings of the study indicated that an increase in MD content resulted in improvements in evaluated properties of the developed composites, including elastic modulus, hardness, fracture toughness, flexural modulus, and strength (including impact, compressive, inter-laminar shear, and flexural strength). Soydal et al. [16] fabricated epoxy/MD composites with a marble content of 0–30 wt%. The authors observed that the incorporation of MD effectively raises the Young's modulus of epoxy while reducing the ductility. Considering the strength of epoxy no significant alteration was found when the concentration of MD did not exceed 20 wt%, above that, however, the strength of the composites decreased. Choudhary and his colleagues [17] prepared ternary composites based on epoxy with glass fiber and marble powder as reinforcement. In their study, the effect of 0–30 wt% MD was analyzed regarding the mechanical and wear properties. The incorporation of waste MD was observed to improve the dynamic mechanical properties of epoxy/glass fiber composites by increasing the storage modulus values. The wear rate of the fabricated samples was also reduced with increasing waste MD content. The literature also demonstrates the impact of waste MD particles on the physical, mechanical, and thermal properties of different polymer matrix composites, including poly(lactic acid) [18,19], high-density polyethylene [20], low-density polyethylene [21], and polypropylene [22].

Nowadays, plastic pollution has emerged as a significant environmental concern, given the exponential growth in the production of disposable plastic items, surpassing the world's capacity to handle them effectively [23]. The optimal approach to address plastic waste is through recycling, which enables the creation of similar products from the original materials for various purposes [24,25]. Incorporating recycled plastics, mainly recycled polyethylene terephthalate (rPET), in multi-component polymeric materials is increasingly favored due to its numerous advantages [26,27]. One such attribute is embodied energy, which measures 27–30 MJ/kg for rPET, whereas primary PET possesses an embodied energy of 78–86 MJ/kg [28]. Consequently, utilizing rPET in product manufacturing allows for approximately 50–60 % energy savings compared to primary PET, attributable to the disparity in embodied energies between primary production and recycling processes [29]. Various waste materials such as sawdust [30], rice husk [31], window glass powder [32], recycled newspaper fibers [33], palm oil fuel ash [34], and fly ash [35] have been reported to influence the mechanical and thermal performance of rPET. However, limited research is available on using waste MD in developing rPET-based composites.

Although in our previous study [36] we investigated the physical, mechanical, and sliding wear properties of MD-filled rPET composites, the impact of MD loading on thermal, thermo-mechanical, and structural features has yet to be explored. Consequently, this study aims to assess the impact of incorporating MD as a filler in rPET for producing composite materials using an extrusion process and injection molding. Fourier transform infrared spectroscopy (FTIR), differential scanning calorimetry (DSC), thermogravimetric analysis (TGA), and dynamic mechanical analysis (DMA) are employed to gain a deeper comprehension of how filler loading affects thermal behavior, including glass transition, melting, and crystallization.

2. Materials and methods

2.1. Materials

Commercially available rPET granules were obtained from Fe-Group Invest Zrt. (Budapest, Hungary). The intrinsic viscosity of the light blue rPET pellets was 0.80 dL/g. The MD used as filler was purchased from Taj Granites Private Ltd. (Jaipur, India). It had a particle size of 5–15 μm, while its density was 2.68 g/cm^3. The scanning electron microscopic image of the MD is shown in Fig. S1 (supplementary materials).

2.2. Fabrication of the samples

As a first step of processing both components were dehumidified in a DEGA-2500 drying unit (Corte Franca, Italy). Throughout the drying – which lasted for a period of 6 h – the temperature was set to 140 °C. The composites were fabricated by melt mixing, carried out using a Labtech LTE 20–44 twin-screw extruder (SamutPrakarn, Thailand). Twin-screw extruders are known to have an excellent mixing capacity; therefore, it was expected that using this machinery would provide a homogenous dispersion of MD particles in the rPET matrix. The diameter of the screws was 20 mm, while their L/D ratio was 44. The rotational speed during the compounding was set to 30 rpm and the temperature of the extruder barrel sections to 250–280 °C. Composites of 0–20 wt% MD content were fabricated this way. The composition (including the gravimetric and volumetric ratios of the components) and designation of the samples are listed in Table 1. The extruded composites were dried once more under the same circumstances as before the extrusion (140 °C for 6 h) and then injection molded with an Arburg Allrounder 420C injection molding machine (Lossburg, Germany) with a screw diameter of 35 mm. The barrel temperature was 255–275 °C. The injection rate was set to 65 cm^3/s, while the injection pressure was 1200 bar. The holding pressure profile was 850-600-250 bar. The residual cooling lasted for 30 s with a mold temperature of 65 °C.

2.3. Characterization and testing

Fourier transform infrared measurements were performed using a Tensor 37 (Bruker, USA) FTIR apparatus equipped with an attenuated total reflectance (ATR) detector, with the following parameters: number of sample spectra: 16; wave number range: 400-4000 cm^{-1}; and resolution: 4 cm^{-1}. FTIR measurements were performed twice for each sample. The presented curves are the averages of the two parallel measurements.

The crystallinity of the materials was investigated using a DSC131 EVO (Setaram, France) differential scanning calorimetric instrument, with samples of 6–8 mg. The heating-cooling-heating cycles were carried out between 30 and 320 °C at a rate of 10 °C/min, with two parallel measurements per sample. The first heating cycle only served the purpose of erasing the thermal history of the samples and the second cycle was applied to analyze the melting behavior and crystallinity. The ratio of crystallinity (X_c) was calculated using Equation (1):

$$X_c = \frac{\Delta H_{mrPET}}{\Delta H^{\infty}_{mrPET} \times \omega_{rPET}} \tag{1}$$

where ΔH_{mrPET} (J/g) is the apparent melting enthalpy of rPET, $\Delta H^{\infty}_{mrPET}$ (J/g) is the melting enthalpy for 100 % crystalline rPET and ω_{rPET} is the weight fraction of rPET in the corresponding composite. The degree of crystallinity was calculated considering an ideal melting enthalpy ($\Delta H^{\infty}_{mrPET}$) of 140 J/g [37].

Thermogravimetric analysis was performed with a LabsysEvo (Setaram, France) analyzer at a heating rate of 20 °C/min in a nitrogen atmosphere in the temperature range of 50–1000 °C, with two parallel measurements per sample. This technique was used to study the thermal stability of the samples by analyzing the mass loss curve and its derivative.

The variation of dynamic mechanical properties was measured with a DMA 25 (Metravib, France) apparatus using a temperature sweep in a tension mode between 0 and 90 °C at a heating rate of 2 °C/min. The gripped length was 20 mm, the frequency was set to 1 Hz and the amplitude was 20 μm. DMA measurements were performed once on each sample. The whole procedure of sample preparation and characterization is shown as a flow chart in Fig. 1.

Table 1
Designation and composition of the prepared composites.

Designation	rPET content [wt.%]	MD content [wt.%]	rPET content [vol%]	MD content [vol%]
rPET	100	0	100	0
rPET_2.5MD	97.5	2.5	98.7	1.3
rPET_5MD	95	5	97.4	2.6
rPET_10MD	90	10	94.6	5.4
rPET_20MD	80	20	88.6	11.4

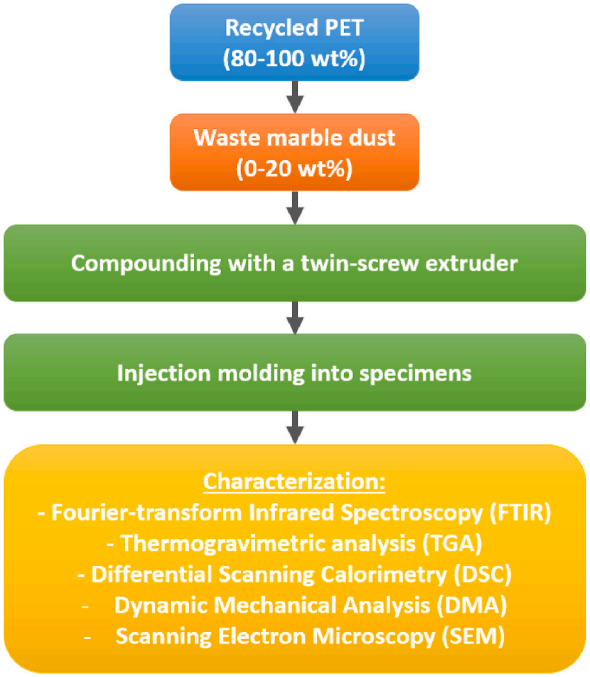

Fig. 1. Flow chart of the rPET/MD composite fabrication and characterization process.

3. Results and discussion

3.1. Structural properties

The presence of marble particles within the rPET matrix was analyzed by ATR FTIR measurements. Fig. 2 represents the ATR FTIR spectra of rPET, MD, and the composites containing 2.5, 5, 10, and 20 wt% marble. Fig. 2a shows the entire analyzed wave number range, while Fig. 2b focuses on the so-called fingerprint region, which is mostly defined between 1800 cm^{-1} and 400 cm^{-1}. The repeating unit of PET chains contains four functional groups, namely an ethyl group, an aromatic ring, and two ester groups [38]. Within the above-described functional groups, the following covalent bonds can be found: C—C, C═C, C—H, C—O, C═O, and aromatic ring.

When examining the FTIR spectrum of unfilled rPET, clear peaks related to the absorption bands appeared at 2962, 1713, 1408, 1338, 1240, 1093, 1014, 872, and 723 cm^{-1}, and there is one additional peak at ~1100 cm^{-1}, which is mostly overlapping with that at 1093 cm^{-1}.According to the literature, the absorption band at 2962 cm^{-1} stands for the asymmetric stretching of the C—H bond. The band at 1713 cm^{-1} is a peak of ester due to the symmetric stretching of the C═O group [39,40]. The peaks at 1408 and 1338 cm^{-1} are

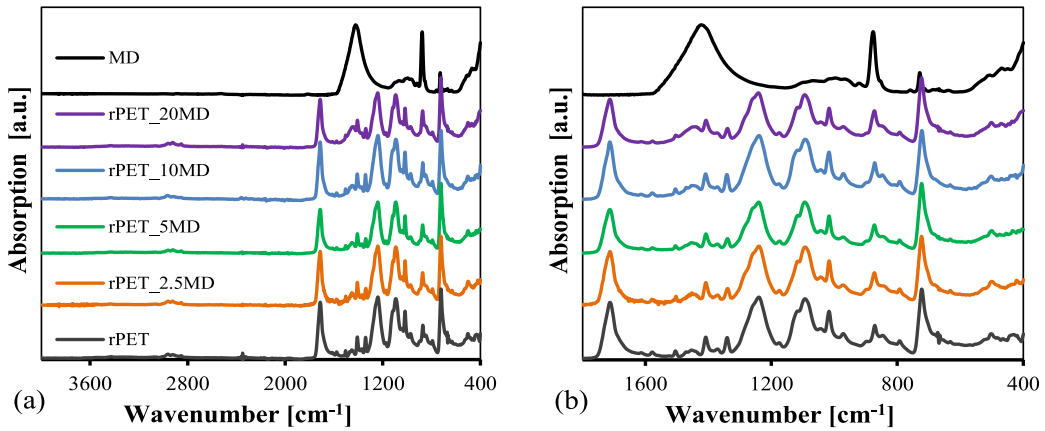

Fig. 2. Complete FTIR spectra of spectra of rPET, marble dust, and their composites with various MD content (a), fingerprint region (b).

attributed to the C—C stretching within the aromatic ring and to the C—O stretch of ester, respectively [40]. The three major peaks at 1240, 1093, and 1014 cm^{-1} represent the stretching of —O—. The peak at ~1100 cm^{-1} – which is present in the form of a shoulder peak of the one at 1093 cm^{-1} – can be ascribed to the out-of-plane stretching of C—H. The band at 872 cm^{-1} corresponds to the para-disubstituted benzene stretching [41], while the peak at 723 cm^{-1} can be assigned to the out-of-plane flexion of the aromatic ring [39].

Meanwhile, the marble powder exhibited three major peaks at 1413, 877, and 727 cm^{-1}, respectively, out of which the first one corresponds to the asymmetric stretching vibration of carbonate radicals, thereby representing the presence of calcite mineral ($CaCO_3$) in the MD as confirmed in previous studies [42,43]. The band at 877 cm^{-1} may either suggest Si–O stretching vibrations or the out-of-plane bending absorption of carbonate ion in $CaCO_3$ according to the literature [43,44], while the band at 727 cm^{-1} can be ascribed to the in-plane bending of calcite [43]. Regarding the rPET/MD composites a combination of the absorption bands exhibited by rPET and MD can be observed, with their intensity being proportional to the ratio of the corresponding component, which suggests no alteration in the chemical structure of the matrix or the filler when being combined through melt mixing.

3.2. Thermal properties

Among the semi-crystalline polymers PET is generally known as a one with rather low crystallization rate, which is disadvantageous when it comes to engineering applications, and therefore, crystallization is often facilitated by incorporating various fillers that act as nucleating agents [45]. Representative heat flow traces recorded during the DSC measurements are depicted in Fig. 3, while the data derived from the curves are collected in Table 2. The curves corresponding to the cooling cycle are shown in Fig. 3a. The DSC trace of unfilled rPET shows a single exothermic transition peaking at 196.7 °C, which represents the crystallization temperature (T_c) of the polymer. When MD was embedded into it, the T_c of rPET gradually shifted to higher temperatures, reaching 204.4 °C for both the rPET_10MD and rPET_20MD samples. This increment in T_c as a function of MD content indicates an earlier crystallization during the cooling process, which can be attributed to a nucleating effect of MD exerted on the polymer. Anis et al. [46] used micro-sized Al particles as a filler for PET, which was also found to facilitate crystallization, while Alshammari et al. [47] incorporated graphite as filler exhibiting the same results. Therefore, it seems straightforward that small-sized rigid particles, including MD, can be used effectively for nucleation in PET composites regardless of whether they are carbonaceous, metallic, or ceramic-based. This kind of behavior is not uncommon for polymer composites of other matrices filled with micron- and nano-sized rigid additives [18].

Fig. 3b shows the second heating curves of the DSC measurement. Apparently, the first change to be observed was a minor shift in the baseline between 65 and 80 °C representing the glass transition (T_g) of rPET. The reason for this baseline shift being rather moderate is the relatively high crystallinity of the samples, which – besides decreasing the ratio of amorphous domains – also facilitates the formation of rigid amorphous (RAF) structures instead of mobile amorphous (MAF) ones. As a consequence, the T_g-s of the samples were evaluated later based on the DMA measurements. With further temperature increase, a rather broad endothermic double peak was found for rPET, corresponding to its melting temperature (T_{m1} and T_{m2}). In the literature, the presence of two overlapping endothermic peaks is either ascribed to the existence of two distinct crystalline polymorphs or a single one containing a certain amount of less regularly oriented chain segments that go through a rearrangement/recrystallization during the melting [48]. For the unfilled rPET matrix, the first melting peak occurred at 240.5 °C and the second one at 249.1 °C, with the second one being the superior in size. With the addition of waste MD, no discernible pattern based on the filler content was observed in the T_m values, suggesting that the marble did not affect the thermal stability. Meanwhile, as a function of MD content, the first melting peak became more and more prominent relative to the second one. Zhao et al. [48] made similar observations for PET-based multi-component materials and claimed that the formation of less regularly oriented chain segments is reasonable when the mobility of the chain molecules is hampered for some reason. It makes sense that the same phenomenon occurred here, since rigid filler particles, such as MD

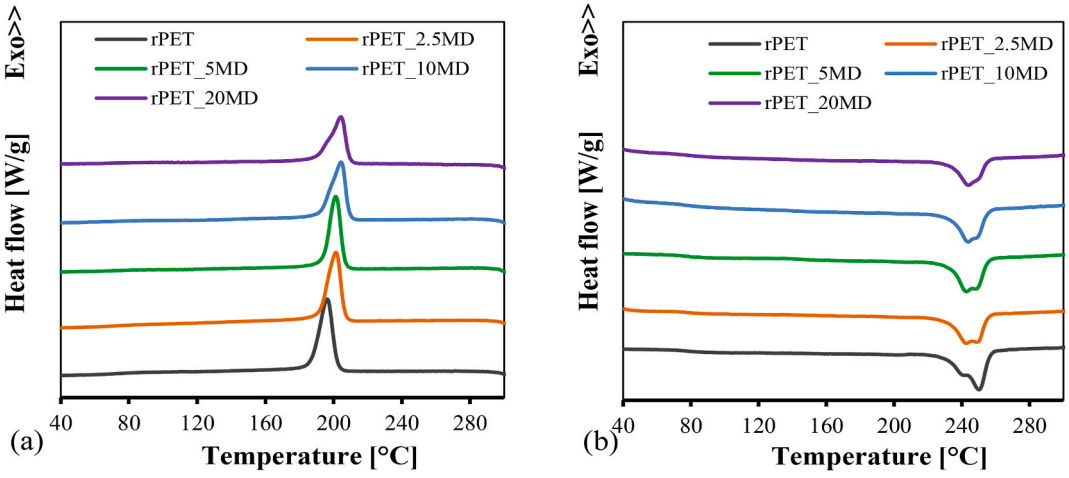

Fig. 3. Crystallization (a) and melting (b) curves of rPET and its MD-filled composites obtained through DSC measurements.

Table 2
Data of unfilled rPET and the rPET/MD composites, derived from DSC curves.

Sample	T_c[°C]	T_{m1}[°C]	T_{m2} [°C]	ΔH_{mrPET}[J/g]	X_c [%]
rPET	196.7	240.5	249.1	33.1	23.7
rPET_2.5MD	201.3	243.0	249.5	30.1	22.1
rPET_5MD	203.6	243.6	249.8	26.2	19.7
rPET_10MD	204.4	244	249.6	26.8	21.2
rPET_20MD	204.4	242.2	248.4	21.5	19.2

incorporated into thermoplastics, indeed tend to reduce molecular mobility.

The crystallinity (X_c) of the samples was calculated using Equation (1) and listed in Table 2. The crystallinity ratio of rPET was determined as 23.7 %, and it slightly decreased in the presence of MD particles, bottoming at 19.2 % for the composite rPET_20MD. This reduction in crystallinity – especially considering the nucleating effect of MD – further supports the assumption that the embedded marble powder hampers the mobility of rPET chain molecules, which at the same time suggests a rather strong interaction between the components.

Fig. 4 shows the TGA thermograms of the fabricated samples. TGA is considered the most favored technique for comparing the thermal stability of different materials. The mass loss of the samples is depicted in Fig. 4a, while its derivative (DTG) can be seen in Fig. 4b. Based on the TGA curve of unfilled rPET a two-step degradation process can be identified, where the initial degradation starts at a relatively low temperature and is followed by a secondary degradation stage at a higher temperature. The most significant weight loss was suffered during the first decomposition process, which took place between 390 and 480 °C. According to the literature, it is associated with the decomposition of chain molecules through an end-group initiated mechanism and then the thermal decomposition of the products formed during the above-mentioned degradation process [49]. The second degradation stage –corresponding to the thermal degradation of the cross-linked carbonaceous structures that were formed during the first stage – started at 500 °C and lasted until 650 °C. After that, the material retained its residual mass of ~20 % even until 1000 °C. This relatively high ash content for PET polymer is typical [50], especially when measured in an inert nitrogen atmosphere, where the thermally stable cross-linked carbonaceous species are less prone to undergo further degradation, making the second degradation step less prominent.

Contrary to neat rPET, the MD-containing composites exhibited a three-step degradation, with the third step corresponding to the thermal decomposition of marble powder. The weight loss of MD was observed in the temperature range of 650 and 770 °C, which is close to those values that were reported in the literature [51]. The mass loss of MD at this elevated temperature can be attributed to the decomposition of $CaCO_3$, which undergoes a reaction upon heating. During this reaction an evolution of CO_2 takes place, and as a result, only calcium oxide remains of $CaCO_3$. Obviously, with increasing MD content the degradation step corresponding to this reaction gets more and more prominent. The TGA data demonstrated almost equal thermal stability of the composites, irrespective of the MD dose. Furthermore, the ash content of the composites exhibited an increase with MD loading, despite the fact that the degradation of rPET took place within the same temperature range. Gao et al. [52] obtained comparable findings using PET composites loaded with $CaCO_3$. The authors claimed that within a certain temperature range of 430.26–431.10 ± 0.82 °C, the ash content of the composites showed a rise as the $CaCO_3$ loadings rose. Thumsorn et al. [53,54] and Chowreddy et al. [55] also found comparable outcomes regarding the thermal stability and heightened ash content of rPET composites when reinforced with $CaCO_3$ particles, hybrid ammonium polyphosphate/talc/glass beads, and carbon nanotubes. Prior studies have shown that the addition of marble particles to other polymeric matrices, such as polypropylene [56] and epoxy [57], enhances the thermal stability and ash content of the resultant composites.

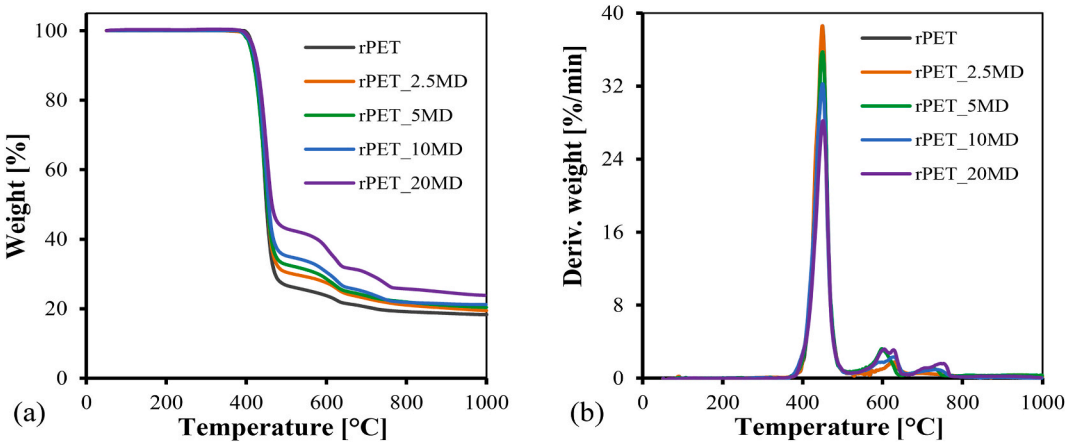

Fig. 4. TGA (a) and DTG curves (b) of rPET and its composites with various MD content.

3.3. Dynamic mechanical properties

Dynamic mechanical analysis (DMA) was carried out on the samples in order to obtain information on the trend of the viscoelastic parameters, namely storage modulus (E'), loss modulus (E''), and loss factor (tan δ), as a function of temperature. Fig. 5a shows the storage modulus versus temperature curves of the prepared samples. For unfilled rPET, the storage modulus was 1936 MPa at 0 °C and it gradually decreased with increasing temperature. A sharp drop in E' was found in the range of 55–80 °C corresponding to the glass transition of the polymer. A similar behavior was observed for the MD-filled composites; however, they exhibited considerably higher storage modulus values. For example, the sample rPET_5MD had an E' of 2150 MPa at 0 °C (relatively 11 % higher than that of rPET), while rPET_20MD showed a value of 2606 MPa at that point (relatively 35 % higher than that of rPET). This pattern aligns with earlier research that documented a rise in the storage modulus of rPET composites when reinforced with glass fibers [58], natural fiber [59], talc particles [60], and carbon nanotubes [55]. The addition of waste marble particles to epoxy [13,61], and waste slate particles to poly(lactic acid) [62], has been shown to enhance the storage modulus of the resultant composites.

The glass transition of the polymers can be better appreciated from the trend of tan δ, (Fig. 5b). The loss factor curve of unfilled rPET showed a double peak with maximum points at 65 °C and 78 °C. Both are in the same temperature range where the DSC curves exhibited a baseline shift corresponding to the T_g. The two distinct peaks refer to a heterogeneous amorphous structure in rPET, which is assumed to be consisting of rigid amorphous (RAF) and free mobile amorphous (MAF) domains. RAF domains typically surround the crystalline segments of the polymer and also any filler or additive incorporated into it [63]. Karayannidis et al. [64] have shown by thermomechanical analysis that two T_g temperatures can be detected for many semi-crystalline polyesters, including PET, with the first one corresponding to MAF and the second one to RAF transformation. This specific behavior is not observed in the DSC thermogram of the same semi-crystalline rPET sample. It is reasonable because the RAF represents the fraction of the amorphous phase that does not contribute to the heat capacity change, therefore it cannot be detected in the calorimetric glass transition. Meanwhile, the RAF may contain chain molecules whose mobility is hindered in the presence of crystallinity or filler.

With increasing marble loading, however, the T_g situated at lower temperature becomes less and less prominent, suggesting that the MAF fraction in the amorphous phase decreases. The probable reason for this is that a strong interfacial connection was formed between the dispersed MD filler and rPET matrix, which also causes the formation of a RAF phase around the filler. This is also in good

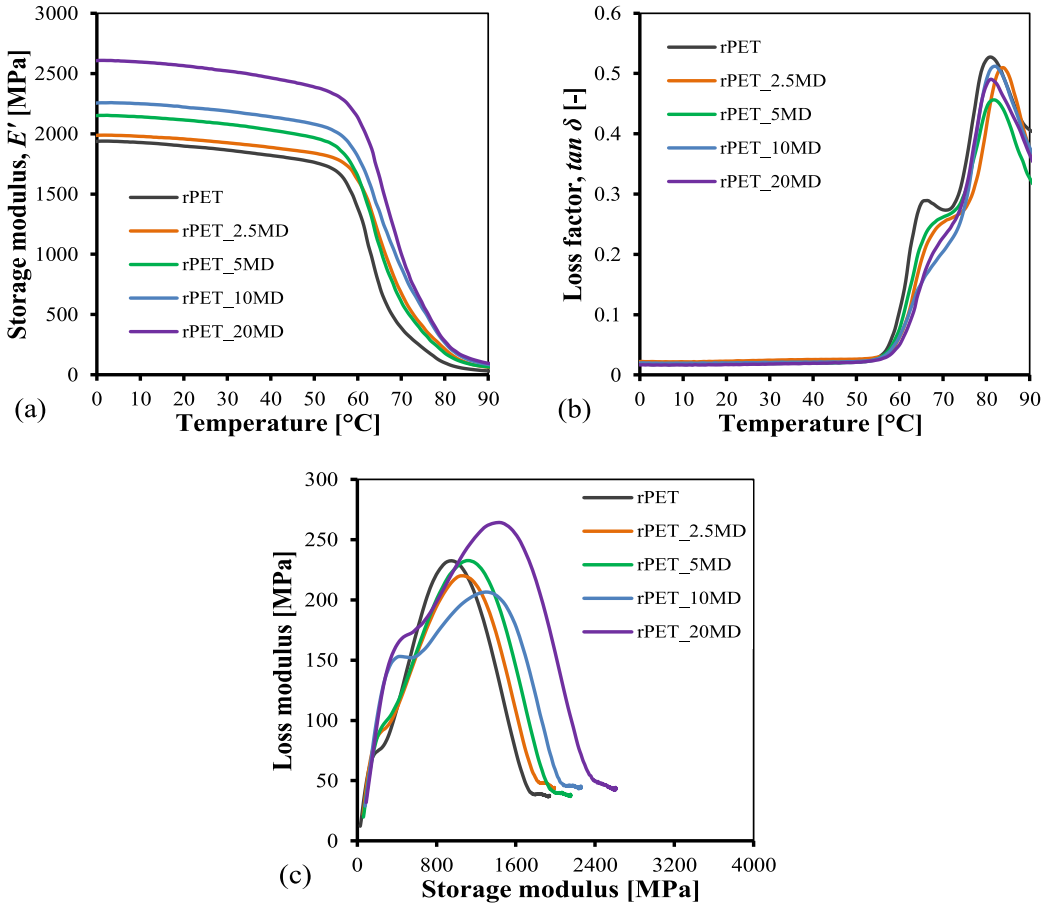

Fig. 5. Storage modulus (a) and loss factor (b) as a function of temperature, and Cole-Cole plot (c) of the fabricated samples.

agreement with the conclusions drawn from the DSC results. As the concentration of MD increases, this RAF volume and the RAF around the crystalline phase together represent an increasing proportion of the amorphous phase. Furthermore, it was observed that the height of the tan δ peak decreased when MD particles were included. The decrease in the peak height of tan δ correlates to the decrease in molecular chain mobility in rPET due to the addition of MD particles. Kumar et al. [61] found similar results in terms of reduced tan δ peak height when examining the influence of MD concentration in epoxy composites. The findings align with previous studies conducted by Pegoretti and Penati [58], Yamada and Thumsorn [60], Chowreddy et al. [55], and Pączkowski et al. [65]. These studies also observed a reduction in the peak height of tan δ for rPET composites reinforced with glass fiber, talc particles, carbon nanotubes, and wood flour, respectively.

The Cole-Cole plot, which was used to analyze the structural changes in composites with the addition of MD particles, indicated the composites' system homogeneity. According to the literature, the homogeneity of the system is determined by the form of the curves, whether elliptical or semicircle [66,67]. As shown in Fig. 5c, the relationship between storage modulus and loss modulus illustrates the characteristics of the composite system. It can be noticed that the curves of the current composite systems' Cole-Cole plots are elliptical. Very excellent adherence between the MD particles and the rPET matrix is indicated by the curve's elliptical or imperfect semicircular shape, and also the qualitative shape of the plots is similar [62,66]. The excellent interaction is also demonstrated through various parameters as seen below. Previous studies have shown comparable findings in Cole-Cole plots for waste slate particles [62] and polymer composites filled with MD [13,61].

Using the storage modulus data, several factors, including the effectiveness factor, degree of entanglement, and reinforcing efficiency factor are calculated to elucidate the reinforcing mechanism of MD within rPET. The efficiency of the reinforcing filler is assessed by the effectiveness factor (E-factor). The efficiency of reinforcement dispersion in the matrix is decreased with a greater E-factor value. Equation (2) can be used to calculate the E-factor [68]:

$$E-factor=\frac{\left(\frac{E'_g}{E'_r}\right)_{composite}}{\left(\frac{E'_g}{E'_r}\right)_{matrix}} \tag{2}$$

where E' denotes the storage modulus and the subscripts r and g denote the rubbery and glassy regions, respectively. For E'_g, the average of E' from the temperature range of 20–30 °C was considered, and for E'_r, the value of the E' at 85 °C was utilized.

The E-factor emphasizes the role of MD loading in the transition from the glassy to the rubbery state, with a lower value indicating more reinforcing efficacy. A lower E-factor was reported for greater MD content in the composite (Fig. 6a), indicating stronger reinforcing effectiveness as MD loading increased. More MD particles in the rPET matrix resulted in improved MD particle/matrix interactions as well as greater particle/particle interactions, resulting in higher stress-transfer between MD particles and matrix and hence reinforcing ability. The results are in line with prior research that found decreased E-factor of various reinforced polymer composites. Incorporating increased wood waste fibers into poly(3-hydroxybutyrate) by Panaitescu et al. [68], graphite flake into acrylonitrile butadiene styrene by Pandey et al. [69], carbon nanotubes into poly(ether ketone) by Chauhan et al. [70], and ramie fiber into polypropylene by He et al. [71] has been shown to decrease the E-factor of the resulting composites.

From the results of E', the degree of entanglement (Φ) between the matrix and reinforcing filler in the polymer composite has also been estimated. Equation (3) may be used to calculate the Φ values [69–71]:

$$\Phi=\frac{E'_r}{6RT} \tag{3}$$

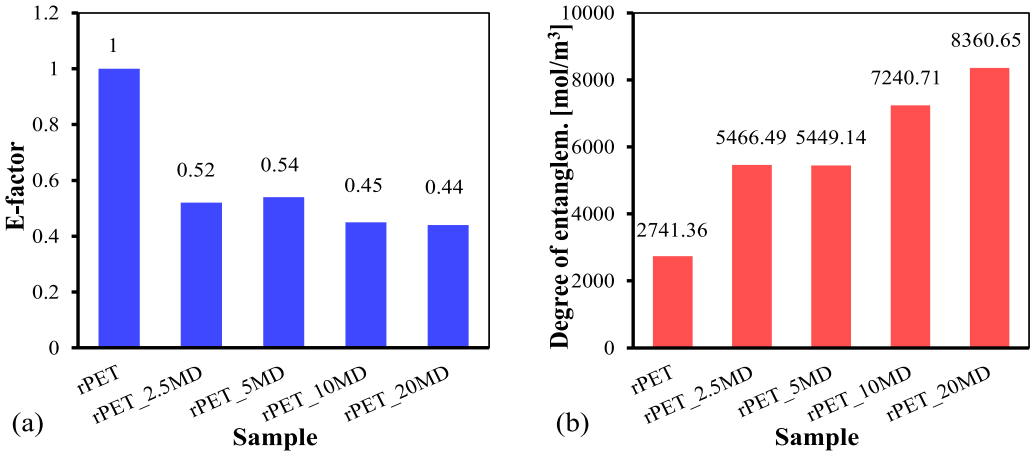

Fig. 6. E-factor (a) and degree of entanglement (b) of the prepared samples.

where, E'_r is the storage modulus in the rubbery region (i.e., 85 °C), R is the universal gas constant and T is the temperature (in Kelvin).

Fig. 6b depicts the computed Φ findings for the examined composites. It has been noticed that Φ increases as the MD content of the composites increases. The chance of interaction among filler particles increases dramatically as the concentration of reinforcement increases, which may lessen the degree of entanglement. However, the behavior of entanglement is growing in nature, implying less contact between filler particles. The pattern is consistent with the storage modulus values. This trend is in line with previous studies that reported an increase in the degree of entanglement of polymer composites reinforced with graphite flake [69], carbon nanotubes [70], and ramie fiber [71].

The reinforcement efficiency factor (R-factor) provides information on filler-matrix bonding by accounting for the effect of fractional filler addition into polymer composites. The R-factor may be calculated using Einstein's equation (4), which is as follows [71,72]:

$$R-factor = \frac{E'_c - E'_p}{E'_p} \times \frac{1}{V_f} \tag{4}$$

where, E' is the storage modulus, and the subscript c and p represent the composite and pure rPET polymer, respectively. The average of E' from the temperature range 20–30 °C was considered for calculation. The symbol V_f denotes the volume proportion of the MD particles.

Fig. 7a shows the computed R-factor for the composites under investigation. The R-factor has been seen to increase for composites up to 5 wt% of MD content, attaining maxima at 5 wt% of MD loading, and then declining when more MD is added. Due to potential MD particle agglomerations, higher MD loadings (>10 wt%) drop the R-factor. He et al. [71] and Jyoti et al. [72] investigated the performance of ramie fiber and carbon nanotube-reinforced polymer composites, likewise noticing an initial increasing trend in R-factor and later a decreasing pattern with increased reinforcement ascribed to its agglomeration. Agglomeration of MD is also present within the samples examined in this current study as seen on scanning electron microscopic (SEM) images in Fig. S2 provided as supplementary materials. Agglomeration of filler particles in polymer composites might be avoided by the introduction of various dispersants; however, using such chemicals would compromise the environmentally friendliness of the developed composites.

The inclusion of reinforcements into the polymer matrix is widely known to severely limit the mobility of polymer chains, which is responsible for stiffness augmentation. The tan δ plot also verifies the stiffness variations in the produced composites. The addition of MD particles, as shown from the tan δ plot, not only causes the tan δ peak to migrate towards higher temperatures but also causes the peak magnitude to decrease. The drop in the tan δ peak implies a decrease in active polymeric chains and an improvement in interface bonding. It may thus be used to estimate the number of polymer chains immobilized *via* matrix-filler interaction using Equation (5) [71,73]:

$$\Delta_v = \frac{\omega_0 - (1-\Delta_0)\omega}{\omega_0} \tag{5}$$

where, Δ_v and ω represent the volume fraction of the immobilized polymer chains and the fraction of energy loss in the composites. The symbols Δ_0 and ω_0 represent the volume fraction of the immobilized chains and the energy loss fraction in pure rPET. Equation (6) may compute the energy loss fraction ω using tan δ at the start of the glass transition region, i.e., 60 °C [71,73]:

$$\omega = \frac{1}{1+\frac{1}{\pi \times tan\ \delta}} \tag{6}$$

In Fig. 7b, the values of Δ_v for various composites are displayed. It should be noted that when the MD content rises, the Δ_v also does.

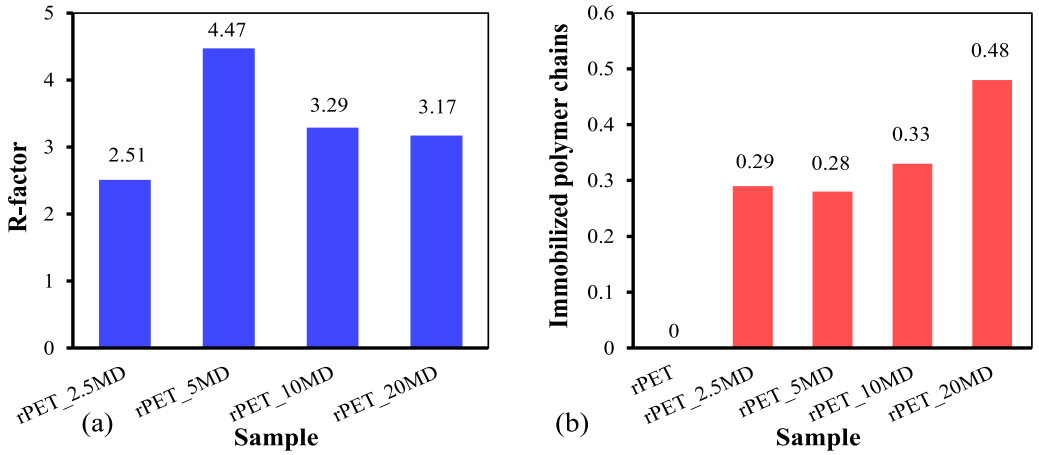

Fig. 7. R-factor (a) and immobilized polymer chains volume fraction (b) of the prepared samples.

This impact is brought about by restricting the polymer matrix by MD particles, which is consistent with the storage modulus trend. Additionally, larger Δ_v values are seen for composites filled with 20 wt% MD, resulting in improved interactions between the filler and the matrix as well as the filler and the filler. This trend is consistent with previous studies by He et al. [71] and Hejna et al. [73] that reported an increase in the immobilized polymer chains fraction of polymer composites reinforced with ramie fiber and agricultural waste, respectively.

In order to attain a deeper comprehension of the interfacial interactions that take place between the MD particles and the rPET matrix, the adhesion factor, also known as the A-factor, was computed by taking the results of the tan δ (peak value) and applying Equation (7) to them [70–73].

$$A - factor = \frac{tan\ \delta_c - tan\ \delta_p}{tan\ \delta_p} \times \frac{1}{1 - V_f} \tag{7}$$

where, tan δ is the loss factor, subscript c and p stand for composite and pure rPET polymers, respectively. The symbol V_f represents the MD particles' volume fraction.

The A-factor values for the composites under investigation are shown in Fig. 8a. Good adhesion and improved interactions between the matrix and low A-factor values indicate reinforcement. Fig. 8a shows that, when compared to an A-factor of 0 for pure rPET, the value of the A-factor drops with growing MD content up to 5 wt% and, after that, increases. The 5 wt% MD reduces the A-factor, an appropriate weight fraction of filler, and lowers composite-to-polymer damping ratios. The potential for interaction between filler particles should grow as the concentration of MD particles ($\geq$10 wt%) increases, raising the A-factor's value. The results are in line with prior research of Panaitescu et al. [68], Pandey et al. [69], and He et al. [71] that reported an initial increasing trend in A-factor which decreased with higher reinforcement concentration.

The interaction between the matrix and fillers impacts dissipation in polymer composites in addition to the matrix. The interphase property between the reinforcing filler and polymer matrix may be identified using the tan δ. The filler-matrix interphase adhesion in polymer composites may be calculated using the B-factor, as shown in Equation (8) [71,72]:

$$B - factor = \frac{tan\ \delta_p - tan\ \delta_c}{tan\ \delta_p} \times \frac{1}{V_f} \tag{8}$$

where tan δ is the loss factor, subscript c and p stand for composite and pure rPET polymers, respectively. While the B-factor is a parameter used to adjust the volume fraction of the reinforcing filler, V_f is the volume fraction of the reinforcing filler.

Fig. 8b depicts the B-factor values for the composites under consideration. The strong interactions between filler and matrix lead to immobilized interphase production, necessitating a volume correction factor (B-factor). The magnitude of interfacial interactions may be inferred from the B-factor value. As the B-factor increases, the immobilized layer thickens, and the interfacial contacts intensify. As shown in Fig. 8b, the highest value of the B-factor in the current investigation occurs at 5 wt% of MD. After that, it gradually goes down as filler-to-filler contact takes over and becomes preponderant. The results are in line with the published literature. Jyoti et al. [72] investigated the performance of carbon nanotube-reinforced polymer composites and likewise noticed an initial increasing trend in the B-factor and later a decreasing pattern with increased reinforcement ascribed to its agglomeration. It is also in good accord with our previous research [36], where the same rPET/MD composites were characterized for their mechanical and morphological properties, and it was found that MD effectively improves the strength of rPET up to 5 wt% filler content. Above that, however, both the tensile and flexural mechanical properties deteriorated due to the agglomeration of the marble particles, which can also be observed in the SEM images of Fig. S2.

4. Conclusions

This work was devoted to studying the structural and thermal properties of polymer composites prepared from rPET as a matrix and waste marble particles as fillers with an MD content of 0–20 wt%. Melt compounding of the composites was performed using a twin-screw extruder and the resulting pellets were then injection molded into suitable specimens. Structural properties of the fabricated samples were investigated through FTIR measurements, while DSC, TGA, and DMA analyses were carried out to investigate their thermal features. Based on the analyses the following conclusions can be drawn:

- The FTIR analysis showed no alteration in the molecular structure of the components.
- The DSC revealed that the MD particles acted as nucleating agents in the rPET, shifting its crystallization (196.7 °C) to higher temperatures ($\Rightarrow$204.4 °C). The marble particles also reduced the mobility of chain molecules, thereby decreasing the overall crystallinity ratio of the polymer.
- According to the TGA measurements there was only a slight increase in the thermal stability of rPET. As a function of MD content, its T_p increased from 446 °C up to 451 °C.
- DMA measurements showed an improved storage modulus of the MD-filled composites in the whole examined temperature range when compared to unfilled rPET. Based on the DMA results, several factors were also determined that indicated a proper adhesion between rPET and MD suggesting a decent reinforcement ability of marble.
- Above 5 wt% MD content, filler-to-filler contact takes over due to agglomeration leading to deteriorating mechanical features. The agglomeration of filler particles was also shown through SEM images.

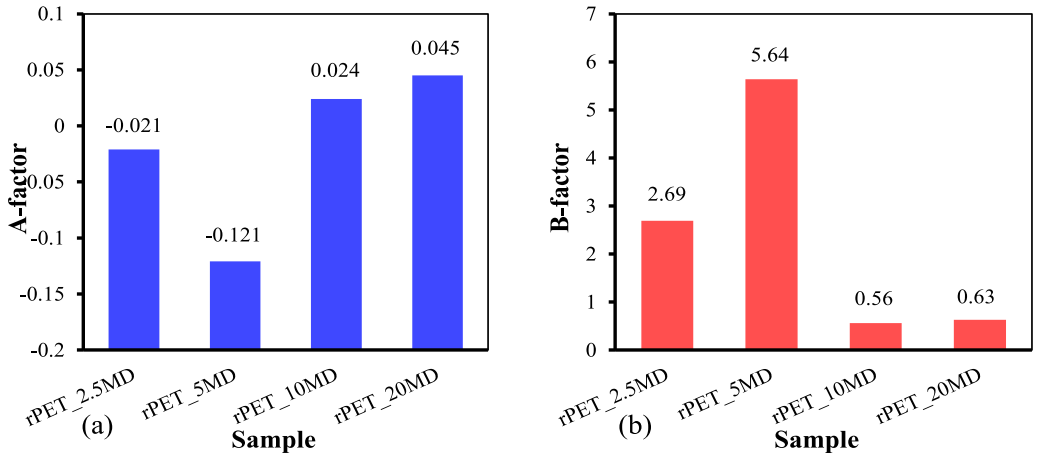

Fig. 8. A-factor (a) and B-factor (b) of the prepared samples.

Data availability statement

The data are available from the corresponding author upon reasonable request.

CRediT authorship contribution statement

László Lendvai: Writing – review & editing, Writing – original draft, Resources, Methodology, Investigation, Formal analysis, Data curation, Conceptualization. **Tej Singh:** Writing – review & editing, Writing – original draft, Resources, Methodology, Investigation, Funding acquisition, Formal analysis, Data curation, Conceptualization. **Ferenc Ronkay:** Writing – review & editing, Methodology, Investigation, Formal analysis, Data curation.

Declaration of competing interest

The authors declare that they have no known competing financial interests or personal relationships that could have appeared to influence the work reported in this paper.

Acknowledgments

The project was supported by the Human Resource Support Operator through the National Talent Programme (Hungary), project nr. NTP-NFTÖ-22-B0199. Project TKP2021-NKTA-48 has been implemented with support provided by the National Research, Development and Innovation Fund (Hungary).

Appendix A. Supplementary data

Supplementary data to this article can be found online at https://doi.org/10.1016/j.heliyon.2024.e25015.

References

[1] M. Fedele, V. Formisano, Waste from criticality to resource through an innovative circular business model: a case study in the manufacturing industry, J. Clean. Prod. 407 (2023) 137143.
[2] R. Naveenkumar, J. Iyyappan, R. Pravin, S. Kadry, J. Han, R. Sindhu, M.K. Awasthi, S.L. Rokhum, G. Baskar, A strategic review on sustainable approaches in municipal solid waste management and energy recovery: role of artificial intelligence, economic stability and life cycle assessment, Bioresour. Technol. 379 (2023) 129044.
[3] F. Haque, C. Fan, Y.-Y. Lee, From waste to value: Addressing the relevance of waste recovery to agricultural sector in line with circular economy, J. Clean. Prod. 415 (2023) 137873.
[4] G. Hondroyiannis, E. Sardianou, V. Nikou, K. Evangelinos, I. Nikolaou, Energy market dynamics and institutional sustainability: how affect the Europe's circular economy, Circular Economy 2 (2023) 100048.
[5] I. Khan, N. Kumar, M. Choudhary, S. Kumar, T. Singh, Mechanical and dynamic mechanical behavior of 3D printed waste slate particles filled acrylonitrile butadiene styrene composites, Arab. J. Chem. 17 (2024) 105559.
[6] A. Danish, M.A. Mosaberpanah, M.U. Salim, R. Fediuk, M.F. Rashid, R.M. Waqas, Reusing marble and granite dust as cement replacement in cementitious composites: a review on sustainability benefits and critical challenges, J. Build. Eng. 44 (2021) 102600.

[7] E. Kuoribo, H. Mahmoud, Utilisation of waste marble dust in concrete production: a scientometric review and future research directions, J. Clean. Prod. 374 (2022) 133872.
[8] B. Basaran, I. Kalkan, C. Aksoylu, Y.O. Özkılıç, M.M. Sabri, Effects of waste powder, fine and Coarse marble Aggregates on concrete compressive strength, Sustainability 14 (21) (2022) 14388.
[9] A. Pappu, V.K. Thakur, R. Patidar, S.R. Asolekar, M. Saxena, Recycling marble wastes and Jarosite wastes into sustainable hybrid composite materials and validation through Response Surface Methodology, J. Clean. Prod. 240 (2019) 118249.
[10] J. Ahmad, F. Aslam, R. Martinez-Garcia, J. de-Prado-Gil, S.M.A. Qaidi, A. Brahmia, Effects of waste glass and waste marble on mechanical and durability performance of concrete, Sci. Rep. 11 (2021) 21525.
[11] M.E. Çınar, F. Kar, Characterization of composite produced from waste PET and marble dust, Construct. Build. Mater. 163 (2018) 734–741.
[12] P. Bakshi, A. Pappu, R. Patidar, M.K. Gupta, V.K. Thakur, Transforming marble waste into high-performance, water-resistant, and thermally insulative hybrid polymer composites for environmental sustainability, Polymers 12 (8) (2020) 1781.
[13] M. Choudhary, T. Singh, M. Dwivedi, A. Patnaik, Waste marble dust-filled glass fiber-reinforced polymer composite Part I: physical, thermomechanical, and erosive wear properties, Polym. Compos. 40 (2019) 4113–4124.
[14] S.K. Nayak, A. Satapathy, Development and characterization of polymer-based composites filled with micro-sized waste marble dust, Polym. Polym. Compos. 29 (5) (2021) 497–508.
[15] A. Sharma, M. Choudhary, P. Agarwal, S.K. Biswas, A. Patnaik, Effect of micro-sized marble dust on mechanical and thermo-mechanical properties of needle-punched nonwoven jute fiber reinforced polymer composites, Polym. Compos. 42 (2021) 881–898.
[16] U. Soydal, S. Kocaman, M. Esen Marti, G. Ahmetli, Study on the reuse of marble and andesite wastes in epoxy-based composites, Polym. Compos. 39 (2018) 3081–3091.
[17] M. Choudhary, T. Singh, A. Sharma, M. Dwivedi, A. Patnaik, Evaluation of some mechanical characterization and optimization of waste marble dust filled glass fiber reinforced polymer composite, Mater. Res. Express 6 (2019) 105702.
[18] L. Lendvai, T. Singh, G. Fekete, A. Patnaik, G. Dogossy, Utilization of waste marble dust in poly(lactic acid)-based biocomposites: mechanical, thermal and wear properties, J. Polym. Environ. 29 (2021) 2952–2963.
[19] T. Singh, P. Pattnaik, D. Shekhawat, L. Ranakoti, L. Lendvai, Waste marble dust-filled sustainable polymer composite selection using a multi-criteria decision-making technique, Arab. J. Chem. 16 (2023) 104695.
[20] A.H. Awad, R. El-Gamasy, A.A. Abd El-Wahab, M.H. Abdellatif, Assessment of mechanical properties of HDPE composite with addition of marble and granite dust, Ain Shams Eng. J. 11 (2020) 1211–1217.
[21] A.H. Awad, M.H. Abdellatif, Assessment of mechanical and physical properties of LDPE reinforced with marble dust, Compos. B Eng. 173 (2019) 106948.
[22] A.H. Awad, R. El-gamasy, A.A. Abd El-Wahab, M. Hazem Abdellatif, Mechanical behavior of PP reinforced with marble dust, Construct. Build. Mater. 228 (2019) 116766.
[23] L.M. Erdle, M. Eriksen, Monitor compartments, mitigate sectors: a framework to deconstruct the complexity of plastic pollution, Mar. Pollut. Bull. 193 (2023) 115198.
[24] N. Ahmed, Utilizing plastic waste in the building and construction industry: a pathway towards the circular economy, Construct. Build. Mater. 383 (2023) 131311.
[25] R.A. Muñoz Meneses, G. Cabrera-Papamija, F. Machuca-Martínez, L.A. Rodríguez, J.E. Diosa, E. Mosquera-Vargas, Plastic recycling and their use as raw material for the synthesis of carbonaceous materials, Heliyon 8 (2022) e09028.
[26] V.A. Szabó, G. Dogossy, Structure and properties of closed-cell foam prepared from rPET, IOP Conf. Ser. Mater. Sci. Eng. 426 (2018) 012043.
[27] V.A. Szabó, G. Dogossy, Flame retardancy of recycled PET foam, IOP Conf. Ser. Mater. Sci. Eng. 903 (2020) 012048.
[28] A.K. Singh, R. Bedi, B.S. Kaith, Composite materials based on recycled polyethylene terephthalate and their properties – a comprehensive review, Compos. B Eng. 219 (2021) 108928.
[29] P. Sarda, J.C. Hanan, J.G. Lawrence, M. Allahkarami, Sustainability performance of polyethylene terephthalate, clarifying challenges and opportunities, J. Polym. Sci. 60 (2022) 7–31.
[30] M. Cosnita, C. Cazan, A. Duta, Interfaces and mechanical properties of recycled rubber–polyethylene terephthalate–wood composites, J. Compos. Mater. 48 (2014) 683–694.
[31] R.S. Chen, S. Ahmad, S. Gan, Rice husk bio-filler reinforced polymer blends of recycled HDPE/PET: three-dimensional stability under water immersion and mechanical performance, Polym. Compos. 39 (2018) 2695–2704.
[32] B.G. Worku, T. Alemneh Wubieneh, Composite material from waste poly (ethylene terephthalate) reinforced with glass fiber and waste window glass filler, Green Chem. Lett. Rev. 16 (2023) 2169081.
[33] S.M. Ardekani, A. Dehghani, M.A. Al-Maadeed, M.U. Wahit, A. Hassan, Mechanical and thermal properties of recycled poly(ethylene terephthalate) reinforced newspaper fiber composites, Fibers Polym. 15 (2014) 1531–1538.
[34] B. Sarde, Y.D. Patil, B.Z. Dholakiya, Evaluation of effectiveness of palm oil fuel ash as green filler and methyl methacrylate as additive in recycled PET resin polymer composite, J. Build. Eng. 43 (2021) 103107.
[35] N.H. Mohd Nasir, F. Usman, A. Saggaf, Saloma, Development of composite material from Recycled Polyethylene Terephthalate and fly ash: four decades progress review, Current Research in Green and Sustainable Chemistry 5 (2022) 100280.
[36] L. Lendvai, F. Ronkay, G. Wang, S. Zhang, S. Guo, V. Ahlawat, T. Singh, Development and characterization of composites produced from recycled polyethylene terephthalate and waste marble dust, Polym. Compos. 43 (2022) 3951–3959.
[37] J.D. Badia, E. Strömberg, S. Karlsson, A. Ribes-Greus, The role of crystalline, mobile amorphous and rigid amorphous fractions in the performance of recycled poly (ethylene terephthalate) (PET), Polym. Degrad. Stabil. 97 (2012) 98–107.
[38] A.A. El-Saftawy, A. Elfalaky, M.S. Ragheb, S.G. Zakhary, Electron beam induced surface modifications of PET film, Radiat. Phys. Chem. 102 (2014) 96–102.
[39] M. Aldas, C. Pavon, H. De La Rosa-Ramírez, J.M. Ferri, D. Bertomeu, M.D. Samper, J. López-Martínez, The impact of biodegradable plastics in the properties of recycled polyethylene terephthalate, J. Polym. Environ. 29 (2021) 2686–2700.
[40] A. Ekinci, M. Öksüz, M. Ates, I. Aydin, Thermal and mechanical properties of polypropylene/post-consumer poly (ethylene terephthalate) blends: bottle-to-bottle recycling, J. Polym. Res. 29 (2022) 433.
[41] M.M. Lubna, K.S. Salem, M. Sarker, M.A. Khan, Modification of thermo-mechanical properties of recycled PET by vinyl acetate (VAc) monomer grafting using gamma irradiation, J. Polym. Environ. 26 (2018) 83–90.
[42] A. Khan, R. Patidar, A. Pappu, Marble waste characterization and reinforcement in low density polyethylene composites via injection moulding: towards improved mechanical strength and thermal conductivity, Construct. Build. Mater. 269 (2021) 121229.
[43] G.-B. Cai, S.-F. Chen, L. Liu, J. Jiang, H.-B. Yao, A.-W. Xu, S.-H. Yu, 1,3-Diamino-2-hydroxypropane-N,N,N′,N′-tetraacetic acid stabilized amorphous calcium carbonate: nucleation, transformation and crystal growth, CrystEngComm 12 (2010) 234–241.
[44] A.K. Jain, A.K. Jha, Shivanshi, Improvement in subgrade soils with marble dust for highway construction: a comparative study, Indian Geotech. J. 50 (2020) 307–317.
[45] X. Zhang, S. Zhao, M.G. Mohamed, S.-W. Kuo, Z. Xin, Crystallization behaviors of poly(ethylene terephthalate) (PET) with monosilane isobutyl-polyhedral oligomeric silsesquioxanes (POSS), J. Mater. Sci. 55 (2020) 14642–14655.
[46] A. Anis, A.Y. Elnour, M.A. Alam, S.M. Al-Zahrani, F. AlFayez, Z. Bashir, Aluminum-filled amorphous-PET, a composite showing simultaneous increase in modulus and impact resistance, Polymers 12 (2020) 2038.
[47] B.A. Alshammari, F.S. Al-Mubaddel, M.R. Karim, M. Hossain, A.S. Al-Mutairi, A.N. Wilkinson, Addition of graphite filler to enhance electrical, morphological, thermal, and mechanical properties in poly (ethylene terephthalate): experimental characterization and material modeling, Polymers 11 (2019) 1411.
[48] Z. Zhao, Y. Wu, K. Wang, Y. Xia, H. Gao, K. Luo, Z. Cao, J. Qi, Effect of the trifunctional chain extender on intrinsic viscosity, crystallization behavior, and mechanical properties of poly(ethylene terephthalate), ACS Omega 5 (2020) 19247–19254.

[49] R.R. Chowreddy, K. Nord-Varhaug, F. Rapp, Recycled poly(ethylene terephthalate)/clay nanocomposites: rheology, thermal and mechanical properties, J. Polym. Environ. 27 (2019) 37–49.
[50] J. Zhang, Q. Ji, P. Zhang, Y. Xia, Q. Kong, Thermal stability and flame-retardancy mechanism of poly(ethylene terephthalate)/boehmite nanocomposites, Polym. Degrad. Stabil. 95 (2010) 1211–1218.
[51] M. Sutcu, H. Alptekin, E. Erdogmus, Y. Er, O. Gencel, Characteristics of fired clay bricks with waste marble powder addition as building materials, Construct. Build. Mater. 82 (2015) 1–8.
[52] W. Gao, X. Ma, Y. Liu, Z. Wang, Y. Zhu, Effect of calcium carbonate on PET physical properties and thermal stability, Powder Technol. 244 (2013) 45–51.
[53] S. Thumsorn, K. Yamada, Y.W. Leong, H. Hamada, Thermal decomposition kinetic and flame retardancy of CaCO3 filled recycled polyethylene terephthalate/recycled polypropylene blend, J. Appl. Polym. Sci. 127 (2013) 1245–1256.
[54] S. Thumsorn, T. Negoro, W. Thodsaratpreeyakul, H. Inoya, M. Okoshi, H. Hamada, Effect of ammonium polyphosphate and fillers on flame retardant and mechanical properties of recycled PET injection molded, Polym. Adv. Technol. 28 (2017) 979–985.
[55] R.R. Chowreddy, K. Nord-Varhaug, F. Rapp, Recycled polyethylene terephthalate/carbon nanotube composites with improved processability and performance, J. Mater. Sci. 53 (2018) 7017–7029.
[56] A.H. Awad, A.W. Abdel-Ghany, A.A. Abd El-Wahab, R. El-Gamasy, M.H. Abdellatif, The influence of adding marble and granite dust on the mechanical and physical properties of PP composites, Journal of Thermal Analysis and Calorimetry 140 (2020) 2615–2623.
[57] V. Fiore, G. Di Bella, T. Scalici, A. Valenza, Effect of plasma treatment on mechanical and thermal properties of marble powder/epoxy composites, Polym. Compos. 39 (2018) 309–317.
[58] A. Pegoretti, A. Penati, Recycled poly(ethylene terephthalate) and its short glass fibres composites: effects of hygrothermal aging on the thermo-mechanical behaviour, Polymer 45 (2004) 7995–8004.
[59] M.A. Kuete, P. Van Velthem, W. Ballout, B. Nysten, J. Devaux, M.K. Ndikontar, T. Pardoen, C. Bailly, Integrated approach to eco-friendly thermoplastic composites based on chemically recycled PET Co-polymers reinforced with treated banana fibres, Polymers 14 (2022) 4791.
[60] K. Yamada, S. Thumsorn, Effectiveness of talc filler on thermal resistance of recycled PET blends, Adv. Mater. Phys. Chem. 3 (8) (2013) 41547.
[61] M. Kumar, R. Kumar, Y. Tak, R.K. Meena, N. Sharma, A. Kumar, Parametric optimization and ranking analysis of hybrid epoxy polymer composites based on mechanical, thermo-mechanical and abrasive wear performance, High Perform. Polym. 33 (2021) 361–382.
[62] I. Khan, k. Neeraj, J.S. Yadav, M. Choudhary, A. Chauhan, T. Singh, Utilization of waste slate powder in poly(lactic acid) based composite for 3D printer filament, J. Mater. Res. Technol. 24 (2023) 703–714.
[63] E. Slezák, F. Ronkay, K. Bocz, Development of an engineering material with increased impact strength and heat resistance from recycled PET, J. Polym. Environ. 31 (2023) 5296–5308.
[64] G. Karayannidis, E. Kirikou, C. Roupakias, G. Papageorgiou, Study of the thermal behaviour of alipharomatic polyesters around the glass–rubber transition region by thermomechanical analysis: the mobile and rigid amorphous fraction, Polym. Int. 56 (2007) 158–166.
[65] P. Pączkowski, A. Puszka, B. Gawdzik, Green composites based on unsaturated polyester resin from recycled poly(ethylene terephthalate) with wood flour as filler-synthesis, characterization and aging effect, Polymers 12 (2020) 2966.
[66] N. Bagotia, D.K. Sharma, Systematic study of dynamic mechanical and thermal properties of multiwalled carbon nanotube reinforced polycarbonate/ethylene methyl acrylate nanocomposites, Polym. Test. 73 (2019) 425–432.
[67] G. Fredi, A. Dorigato, M. Bortolotti, A. Pegoretti, D.N. Bikiaris, Mechanical and functional properties of novel biobased poly(decylene-2,5-furanoate)/carbon nanotubes nanocomposite films, Polymers 12 (2020).
[68] D.M. Panaitescu, C.A. Nicolae, A.R. Gabor, R. Trusca, Thermal and mechanical properties of poly(3-hydroxybutyrate) reinforced with cellulose fibers from wood waste, Ind. Crop. Prod. 145 (2020) 112071.
[69] A.K. Pandey, R. Kumar, V.S. Kachhavah, K.K. Kar, Mechanical and thermal behaviours of graphite flake-reinforced acrylonitrile–butadiene–styrene composites and their correlation with entanglement density, adhesion, reinforcement and C factor, RSC Adv. 6 (2016) 50559–50571.
[70] S.S. Chauhan, B.P. Singh, R.S. Malik, P. Verma, V. Choudhary, Detailed dynamic mechanical analysis of thermomechanically stable melt-processed PEK–MWCNT nanocomposites, Polym. Compos. 39 (2018) 2587–2596.
[71] L. He, F. Xia, Y. Wang, J. Yuan, D. Chen, J. Zheng, Mechanical and dynamic mechanical properties of the amino silicone oil emulsion modified ramie fiber reinforced composites, Polymers (2021) 13.
[72] J. Jyoti, B.P. Singh, A.K. Arya, S.R. Dhakate, Dynamic mechanical properties of multiwall carbon nanotube reinforced ABS composites and their correlation with entanglement density, adhesion, reinforcement and C factor, RSC Adv. 6 (2016) 3997–4006.
[73] A. Hejna, K. Formela, M.R. Saeb, Processing, mechanical and thermal behavior assessments of polycaprolactone/agricultural wastes biocomposites, Ind. Crop. Prod. 76 (2015) 725–733.